

J/ψ production in a gluon plasma produced in Au-Au collisions at the Relativistic Heavy Ion Collider

Bin Zhang and Donald L. Johnson

*Department of Chemistry and Physics,
Arkansas State University, P.O. Box 419,
State University, Arkansas 72467-0419, USA*

(Dated: March 20, 2004)

Abstract

Centrality dependence of J/ψ production in Au-Au collisions at $\sqrt{s_{NN}} = 200$ GeV is studied using the Glauber model plus the kinetic formation model. Initial J/ψ production and destruction by incoming nucleons are described by the Glauber model. J/ψ -charm equilibration in the gluon plasma is described by the kinetic formation model. We explore the possibility of J/ψ suppression suggested by the recent PHENIX data. We show that the J/ψ yield monotonically decreases with increasing centrality in the kinetic formation model when the charm mass is smaller than a critical mass. The final J/ψ yield is between the value after the Glauber suppression and the dynamical equilibrium value. This underscores the importance of both J/ψ production from d-Au collisions, which is essential in determining the Glauber suppression, and high statistics Au-Au data, which can further constrain final state J/ψ -charm equilibration.

PACS numbers: 25.75.-q,24.85.+p,14.40.Lb

I. INTRODUCTION

Relativistic heavy ion collisions have been used for the search of the Quark-Gluon Plasma, a deconfined nuclear matter that is believed to have existed at about one micro-second after the big-bang [1, 2, 3]. The existence and properties of the Quark-Gluon Plasma are reflected in the particle spectra produced in these collisions. One important particle that is sensitive to the Quark-Gluon Plasma production is the J/ψ particle. As color screening in the Quark-Gluon Plasma can dissociate the J/ψ particle, J/ψ suppression relative to the yield from the superposition of nucleon-nucleon collisions can be used as a signal of the production of the Quark-Gluon Plasma [4].

In realistic collisions, the J/ψ particle can also be destructed by incoming nucleons in the colliding nuclei. This is shown clearly by the proton-nucleus collision data [5, 6, 7] where hot and dense nuclear matter is not expected to be produced. Collisions between the J/ψ particle and comovers produced in heavy ion collisions can further modify the J/ψ yield [8, 9, 10, 11, 12, 13, 14, 15, 16, 17, 18, 19, 20, 21]. Hence detailed phenomenological models are necessary for the interpretation of J/ψ production data. By comparing theoretical expectations and experimental results, an abnormal J/ψ suppression in Pb-Pb collisions at the Super-Proton-Synchrotron (SPS) [22] has been identified which indicates the production of hot and dense nuclear matter at the SPS energies.

At the Relativistic Heavy Ion Collider (RHIC) energies, there are on average more than one charm-anti-charm quark pair produced in each event. This opens the possibility of producing the J/ψ particle in the deconfined phase via the reaction $c + \bar{c} \rightarrow J/\psi + g$ [23]. Other possibilities involving J/ψ equilibration at the hadronization time have also been proposed [24, 25, 26]. Many interesting studies have been made on the phenomenological consequences of different production mechanisms [27, 28, 29, 30, 31, 32, 33, 34]. It was demonstrated by the kinetic formation model that at collider energies, due to charm recombination, J/ψ enhancement may be the signal of Quark-Gluon Plasma production, in contrast to the traditional J/ψ suppression scenario. Recently, data on J/ψ production at RHIC have been released [35, 36]. No significant J/ψ enhancement was observed.

In this paper, we will explore the possibility of J/ψ suppression in the framework of the kinetic formation model. In particular, we make the following variations of the original kinetic formation model.

- (1) Recent perturbative Quantum Chromodynamics (QCD) studies of the charmonium spectrum [37, 38, 39, 40] give a charm mass $m_c^{\overline{\text{MS}}}(m_c^{\overline{\text{MS}}}) = 1.243$ GeV, different potential models [41] give $m_c = 1.5$ GeV to $m_c = 1.8$ GeV, preturbative QCD studies of charm production [42, 43] in hadron collisions give a charm mass from $m_c = 1.3$ GeV to $m_c = 1.5$ GeV, a recent Nambu-Jona-Lasinio model calculation [34] gives $m_c = 1.6 - 1.7$ GeV. We will vary the charm quark mass between 1.3 GeV and 1.9 GeV to study the effect of the threshold of J/ψ production on J/ψ -charm equilibration.
- (2) J/ψ break-up cross section by a gluon was calculated in perturbative QCD [44, 45]. The final state is a pair of charm and anti-charm quarks and the cross section decreases with the center-of-mass energy of the J/ψ -gluon system. As the energy increases, the break-up is accompanied by additional parton radiation. We will model this effect by using a J/ψ break-up cross section that is a constant in energy and varies between 1 mb and 6 mb and compare this with the dipole cross section results.
- (3) The original kinetic formation model uses an averaged uniform parton density in the transverse plane. This may underestimate charm-equilibration. In the following, we will use the Glauber model to study particle production and this leads to a better description of the evolution by local temperatures.
- (4) We make use of the recent discovery by the PHENIX collaboration and various theoretical approaches [46, 47, 48, 49, 50, 51, 52, 53] that there is no strong charm energy loss in relativistic nuclear collisions. We also use the recent PHENIX J/ψ data in pp collisions [35] to normalize our calculations.

In the next section, the Glauber model and the kinetic formation model will be introduced. We will use the Glauber model to describe the destruction of initial J/ψ 's by incoming nucleons and use the kinetic formation model to describe J/ψ equilibration in the Quark-Gluon Plasma. The results will be presented in section III. Then we will discuss the implications of our study.

II. THE GLAUBER MODEL AND THE KINETIC FORMATION MODEL

In nucleus-nucleus collisions, initial J/ψ 's are produced by the collisions between incoming nucleons. Once a J/ψ is produced, other nucleons following the collision that produces the

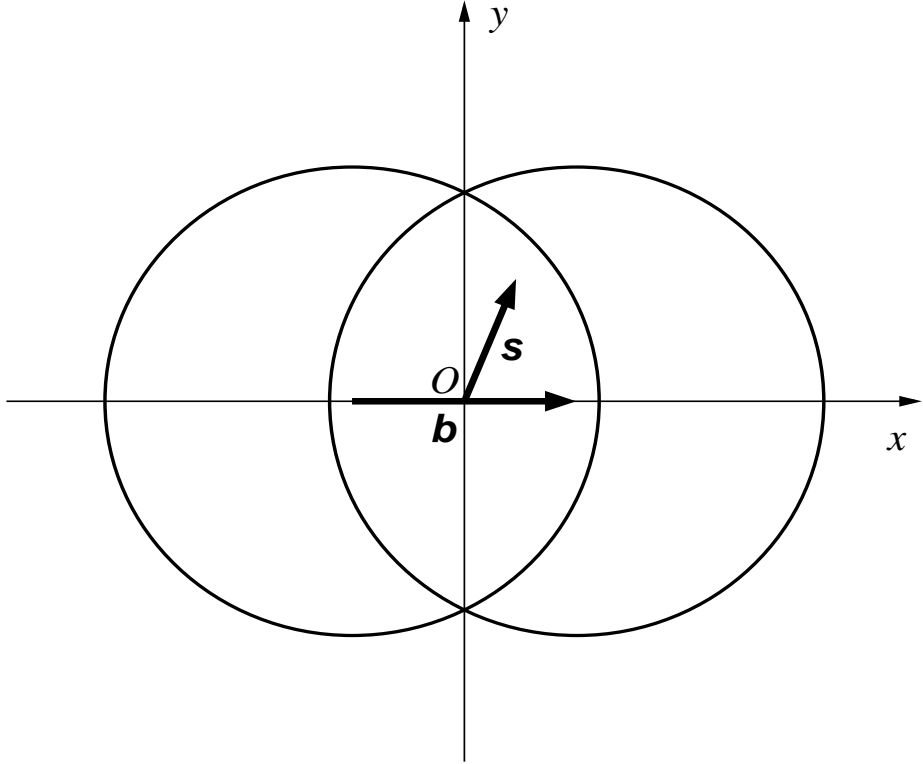


FIG. 1: Nucleus-nucleus collision transverse geometry. The reaction plane is determined by the x -axis that goes along the impact parameter vector \vec{b} and the z -axis that goes along the beam direction. In this figure, the z -axis points out of the paper. The transverse position vector \vec{s} starts at the center of the overlapping region.

J/ψ will have opportunities to collide with it and turn it into a charm-anti-charm pair. The number of J/ψ 's that are produced by collisions between incoming nucleons and survive further collisions with other nucleons can be written as

$$N_{AB \rightarrow J/\psi}(b) = \int d\vec{s} \sigma_{NN \rightarrow J/\psi} t_A(\vec{s} + \frac{\vec{b}}{2}) t_B(\vec{s} - \frac{\vec{b}}{2}) S_A(\vec{s} + \frac{\vec{b}}{2}) S_B(\vec{s} - \frac{\vec{b}}{2}). \quad (1)$$

In the above formula, \vec{b} is the impact parameter vector, and \vec{s} is the transverse position. They are shown in Fig. 1 along with the transverse coordinate system. $\sigma_{NN \rightarrow J/\psi}$ is the J/ψ production cross section in nucleon-nucleon collisions. t_A and t_B are the nuclear thickness functions of nucleus A and nucleus B, while S_A and S_B are the average survival probabilities of a J/ψ after passing through nucleons in nucleus A and nucleus B. The normalization by the probability of a nucleus-nucleus collision at impact parameter b , $\sigma_{AB}(b)$, is not included as it only affects very peripheral events.

We will focus on J/ψ production in Au-Au collisions. To simplify the calculations, a

nucleus is taken to be a hard sphere with uniform nucleon density ρ_N inside, and the radius is determined by $R = r_0 A^{1/3}$ ($r_0 = 1.12$ fm and A is the number of nucleons inside the nucleus). The number of survived J/ψ 's can now be written as:

$$N_{AuAu \rightarrow J/\psi}(b) = \frac{\sigma_{NN \rightarrow J/\psi}}{\sigma_{J/\psi N}^2} \int d\vec{s} (1 - \exp(-2\rho_N \sigma_{J/\psi N} z_0)) (1 - \exp(-2\rho_N \sigma_{J/\psi N} z'_0)), \quad (2)$$

where $\sigma_{J/\psi N}$ is the J/ψ break-up cross section due to the collision with an incoming nucleon and $2z_0$ ($2z'_0$) is the longitudinal length of the row of nucleons inside nucleus A (B) at transverse position (x, y) . More explicitly, $z_0 = \sqrt{R^2 - (x + \frac{b}{2})^2 - y^2}$, and $z'_0 = \sqrt{R^2 - (x - \frac{b}{2})^2 - y^2}$. The transverse position integration $\int d\vec{s}$ becomes $\int dx dy$ over the region $(x + \frac{b}{2})^2 + y^2 < R^2$ and $(x - \frac{b}{2})^2 + y^2 < R^2$.

After the passing of the two incoming nuclei, the J/ψ is immersed in the Quark-Gluon Plasma. As the initial gluon number is much larger than the initial quark number at RHIC energies [54, 55], and in addition, light quark chemical equilibration time is much longer than the expansion time [56], the plasma will be approximated as a gluon plasma. As charm regeneration in the plasma is [57, 58, 59] negligible, charm quark number will be kept constant. There are indications that charm quark thermal equilibration may be possible [60], and we will assume local thermal equilibrium.

J/ψ equilibration in the plasma is achieved through the reaction $J/\psi g \rightarrow c\bar{c}$ and its inverse reaction $c\bar{c} \rightarrow J/\psi g$. Assume the rapidity distributions are flat and focus on one fireball within one unit of rapidity, the J/ψ number $N_{J/\psi}$ satisfies

$$\frac{dN_{J/\psi}}{d\tau} = \lambda_F N_c \rho_{\bar{c}} - \lambda_D N_{J/\psi} \rho_g. \quad (3)$$

In the above, τ is the proper time, N_c is the number of charm quarks per unit rapidity. $\rho_{\bar{c}}$ is the density of anti-charm quarks and it equals the density of charm quarks, ρ_c . ρ_g is the density of gluons.

λ_F is the reduced J/ψ formation rate through the reaction $c\bar{c} \rightarrow J/\psi g$. It equals $\langle \sigma_{c\bar{c} \rightarrow J/\psi g} v_{rel, c\bar{c}} \rangle$, where $\langle \dots \rangle$ denotes average over charm and anti-charm quarks, and $v_{rel, c\bar{c}}$ is the relative speed between a charm quark and an anti-charm quark. When the evolution is in thermal equilibrium, i.e., the evolution is controlled by one temperature T ,

$$\lambda_F = \frac{1}{(2\alpha_c^2 K_2(\alpha_c))^2} \int_{z_0}^{\infty} dz (z^2 - 4\alpha_c^2) z^2 K_1(z) \sigma_{c\bar{c} \rightarrow J/\psi g}(s = z^2 T^2). \quad (4)$$

We use α_c to stand for the mass of charm quark divided by the temperature, i.e., $\alpha_c = m_c/T$. $z_0 = \max(\alpha_c + \alpha_{\bar{c}}, \alpha_{J/\psi} + \alpha_g)$. $K_n(x)$ is the n th order modified Bessel function. s is the center of mass energy squared.

Similarly, λ_D , the reduced J/ψ destruction rate via the reaction $J/\psi g \rightarrow c\bar{c}$ can be written as

$$\lambda_D = \frac{1}{8\alpha_{J/\psi}^2 K_2(\alpha_{J/\psi})} \int_{z_0}^{\infty} dz (z^2 - \alpha_{J/\psi}^2)^2 K_1(z) \sigma_{J/\psi g \rightarrow c\bar{c}}(s = z^2 T^2). \quad (5)$$

The detailed balance relation,

$$\sigma_{c\bar{c} \rightarrow J/\psi g}(s) = \frac{d_{J/\psi g}}{d_{c\bar{c}}} \frac{(k_{J/\psi g})^2}{(k_{c\bar{c}})^2} \sigma_{J/\psi g \rightarrow c\bar{c}}(s), \quad (6)$$

relates the two reduced rates. In Eq. (6), $d_{J/\psi g} = 48$ is the number of degrees of freedom for the $J/\psi g$ system, and $d_{c\bar{c}} = 36$ is the number of degrees of freedom of the $c\bar{c}$ system. $k_{J/\psi g}$ and $k_{c\bar{c}}$ are the center-of-mass momenta of the $J/\psi g$ and $c\bar{c}$ systems. After using the detailed balance relation, we can rewrite λ_F as,

$$\begin{aligned} \lambda_F &= \frac{d_{J/\psi g}}{d_{c\bar{c}}} \frac{1}{(2\alpha_c^2 K_2(\alpha_c))^2} \int_{z_0}^{\infty} dz (z^2 - \alpha_{J/\psi}^2)^2 K_1(z) \sigma_{J/\psi g \rightarrow c\bar{c}}(s = z^2 T^2) \\ &= \frac{d_{J/\psi g}}{d_{c\bar{c}}} \frac{2\alpha_{J/\psi}^2 K_2(\alpha_{J/\psi})}{\alpha_c^4 K_2^2(\alpha_c)} \lambda_D. \end{aligned} \quad (7)$$

In Eq. (3), $N_c = N_{c,0} - N_{J/\psi}$ where $N_{c,0}$ is the number of charm quarks per unit rapidity at the initial time τ_0 . $\rho_c = N_c/V(\tau)$. We use the Bjorken model [61] for the evolution and the volume $V(\tau) = V_0 \tau / \tau_0$. The gluon density $\rho_g = \frac{g_g}{\pi^2} \zeta(3) T^3 \approx 1.95 T^3 = 1.95 \frac{\tau_0 T_0^3}{\tau}$.

III. J/ψ PRODUCTION AT $\sqrt{s_{NN}} = 200$ GEV

A. Initial conditions

The initial gluon number, charm-anti-charm quark number, and J/ψ number for central ($b = 0$) Au-Au collisions will be specified. For non-zero impact parameters, the total number of gluons and the total number of charm-anti-charm quarks follow binary collision scaling, and the J/ψ number follows Eq. (1,2). The transverse density per unit rapidity of gluons (charm-anti-charm pairs) at impact parameter \vec{b} and position \vec{s} is proportional to $t_{Au}(\vec{s} + \frac{\vec{b}}{2}) t_{Au}(\vec{s} - \frac{\vec{b}}{2})$ and is given by

$$\frac{dN_{g(c)}}{dy d\vec{s}}(\vec{b}, \vec{s}) = 4\rho_N^2 z_0 z'_0 \frac{1}{T_{AuAu}(b=0)} \frac{dN_{g(c)}}{dy}(b=0), \quad (8)$$

where $T_{AuAu}(b = 0)$ is the nuclear thickness function at zero impact parameter. It equals $\int d\vec{s} t_{Au}(\vec{s} + \frac{\vec{b}}{2}) t_{Au}(\vec{s} - \frac{\vec{b}}{2}) = 4\rho_N^2 \int d\vec{s} (R^2 - s^2) = \frac{9}{8\pi} \frac{A^{4/3}}{r_0^2}$ with $A = 197$ for Au nucleus. The initial temperatures are local and calculated from the initial gluon density distribution. The J/ψ transverse density per unit rapidity needs additional correction factor $S_{Au}(\vec{s} + \frac{\vec{b}}{2}) S_{Au}(\vec{s} - \frac{\vec{b}}{2})$. It can be written as

$$\frac{dN_{J/\psi}}{dy d\vec{s}}(\vec{b}, \vec{s}) = 4\rho_N^2 z_0 z'_0 \frac{1}{T_{AuAu}(b = 0)} \frac{dN_{J/\psi}}{dy}(b = 0) F(2\rho_N \sigma_{J/\psi N} z_0) F(2\rho_N \sigma_{J/\psi N} z'_0), \quad (9)$$

where function $F(x) = \frac{1 - \exp(-x)}{x}$. The initial time is taken to be $\tau_0 = 0.2$ fm/c. In central collisions, the initial gluon rapidity density is $\frac{dN_g}{dy} = 300$ and charm rapidity density is $\frac{dN_c}{dy} = 2.5$. They are in line with perturbative Quantum Chromodynamics (QCD) based calculations [42, 62, 63]. The initial J/ψ rapidity density before correcting for the Glauber suppression is $\frac{dN_{J/\psi}}{dy} = 0.033$. This value comes from the superposition of J/ψ production from nucleon-nucleon collisions at $\sqrt{s_{NN}} = 200$ GeV using the production cross section measured by the PHENIX collaboration [35] and the nuclear thickness function at zero impact parameter. The J/ψ mass is fixed at $m_{J/\psi} = 3.1$ GeV. The charm quark mass m_c will be varied between 1.3 GeV and 1.9 GeV. The freeze-out temperature T_f is taken to be 0.15 GeV.

B. Cross sections

The J/ψ -nucleon dissociation cross section $\sigma_{J/\psi N}$ will be varied among 0, 4.4 mb, and 7.1 mb [10, 11, 64, 65, 66]. The $J/\psi g \rightarrow c\bar{c}$ cross section is taken to be a constant. We will vary $\sigma_{J/\psi g \rightarrow c\bar{c}}$ to study J/ψ -charm equilibration. A comparison with the results from a dipole cross section will be made to study the effect of the energy dependence of the cross section.

Fig. (2) shows the J/ψ production and destruction cross sections as functions of the center-of-mass energy squared s . In Fig.'s (2a)-(2c), $\sigma_{J/\psi g \rightarrow c\bar{c}}$ is kept at a constant value of 3 mb, which is about the J/ψ size in the vacuum. The inverse cross section, $\sigma_{c\bar{c} \rightarrow J/\psi g}$, depends on the charm quark mass. When the charm quark mass $m_c = 1.5$ GeV, which is smaller than the J/ψ production threshold, the inverse cross section starts at zero and increases with s . It crosses the destruction cross section at $s \approx 40$ GeV². However, when $m_c = 1.7$ GeV, which is larger than the J/ψ production threshold, there is a peak at the

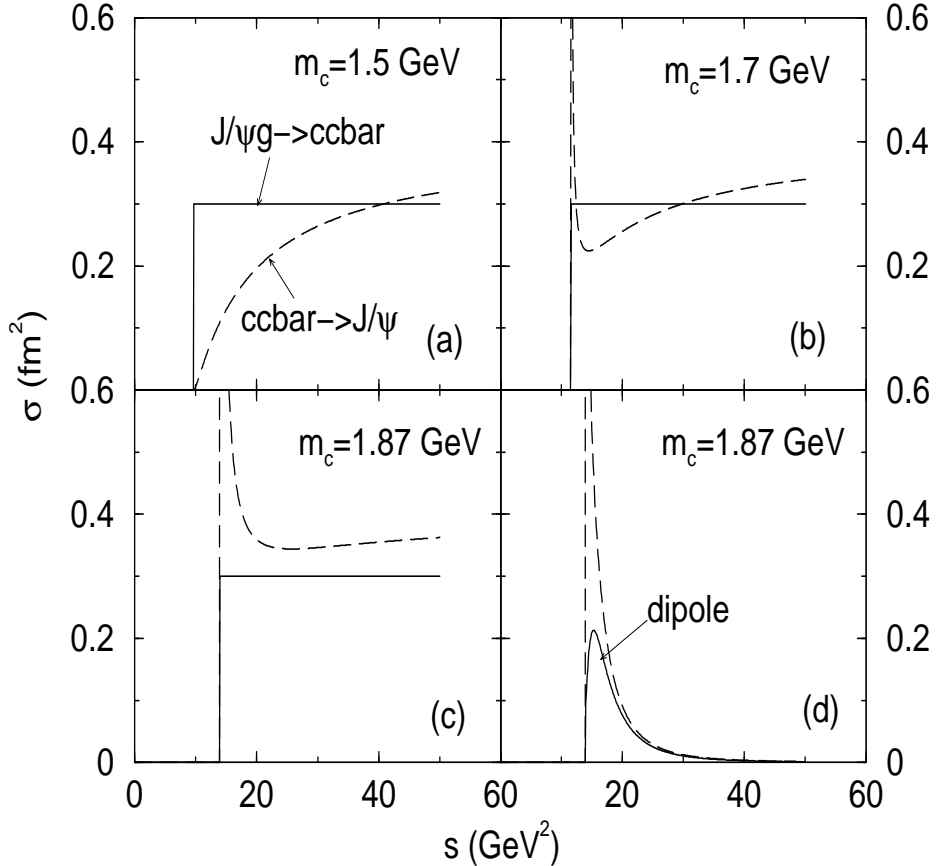


FIG. 2: The J/ψ production and destruction cross sections in a gluon plasma as functions of the center-of-mass energy squared s . In (a)-(c), $\sigma_{J/\psi g} = 3$ mb. In (d), $\sigma_{J/\psi g}$ is specified in Eq. (10).

threshold. When s increases above the threshold, $\sigma_{c\bar{c} \rightarrow J/\psi g}$ first decreases to below $\sigma_{J/\psi g \rightarrow c\bar{c}}$. It then increases and crosses $\sigma_{J/\psi g \rightarrow c\bar{c}}$ at $s \approx 30$ GeV. The width of the peak at the threshold depends on the charm quark mass. The larger the mass, the wider the peak. This can be seen by comparing $\sigma_{c\bar{c} \rightarrow J/\psi g}$ for $m_c = 1.7$ GeV in Fig. (2b) with $\sigma_{c\bar{c} \rightarrow J/\psi g}$ for $m_c = 1.87$ GeV in Fig. (2c). In addition, when m_c increases, the crossing position decreases. Eventually, $\sigma_{c\bar{c} \rightarrow J/\psi g}$ is always larger than $\sigma_{J/\psi g \rightarrow c\bar{c}}$ as shown in Fig. (2c). We also plot the $J/\psi g \rightarrow c\bar{c}$ cross section based on a perturbative QCD calculation [44, 45],

$$\sigma_{J/\psi g \rightarrow c\bar{c}} = \frac{2\pi}{3} \left(\frac{32}{3}\right)^2 \left(\frac{2\mu}{\epsilon_0}\right)^{1/2} \frac{1}{4\mu^2} \frac{(k/\epsilon_0 - 1)^{3/2}}{(k/\epsilon_0)^5}, \quad (10)$$

and its inverse cross section in Fig. (2d). In the above equation, $\mu = m_c/2$ is the reduced charm quark mass in the charm-anti-charm center-of-mass system. k is the gluon

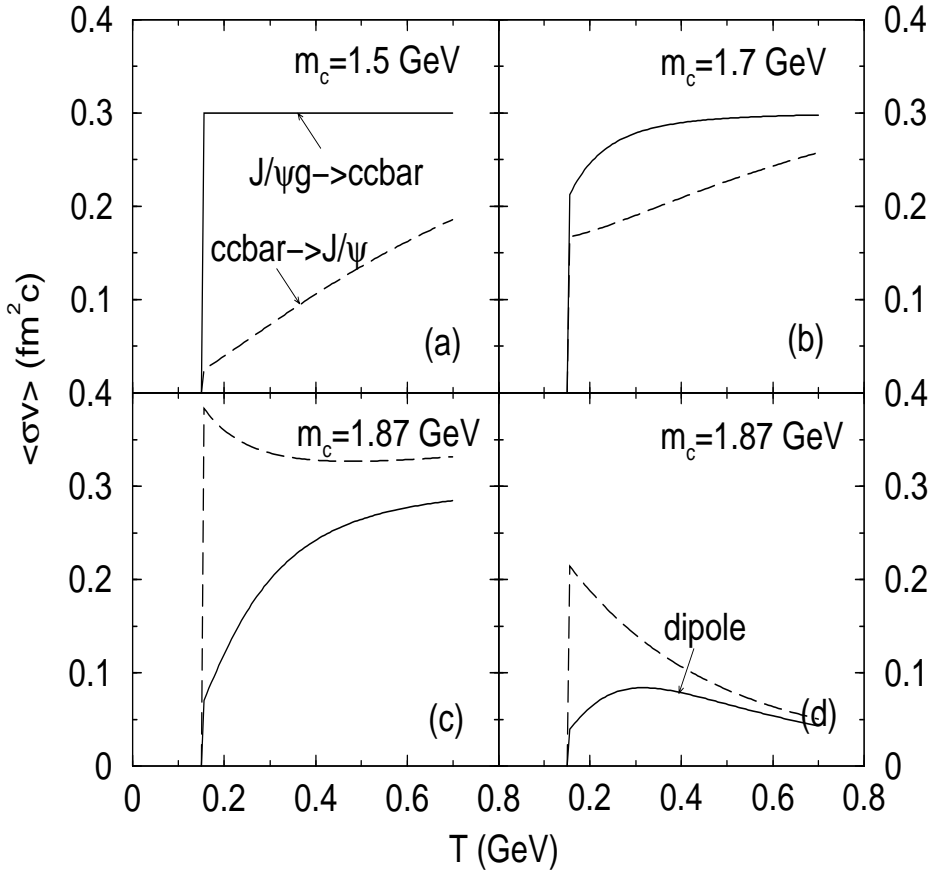


FIG. 3: The reduced reaction rates, $\langle \sigma_{J/\psi g \rightarrow c\bar{c}} v \rangle$ and $\langle \sigma_{c\bar{c} \rightarrow J/\psi} v \rangle$, as functions of the temperature of the plasma.

momentum, and $\epsilon_0 = 2m_c - m_{J/\psi}$ is the binding energy of J/ψ . For m_c equals the D meson in vacuum mass 1.87 GeV, the J/ψ destruction cross section has a finite peak near the threshold. The peak of the cross section is about 2 mb. The production has an infinite peak at the threshold, and it is always larger than the destruction cross section.

The reduced J/ψ production rate $\langle \sigma_{c\bar{c} \rightarrow J/\psi} v \rangle$ and destruction rate $\langle \sigma_{J/\psi g \rightarrow c\bar{c}} v \rangle$ for different cross section choices are plotted in Fig. (3). For m_c smaller than the J/ψ production threshold, when $\sigma_{J/\psi g \rightarrow c\bar{c}}$ is a constant, the reduced J/ψ destruction rate is always a constant and it equals $\sigma_{J/\psi g \rightarrow c\bar{c}} c$. In Fig.'s (3a)-(3c), $\sigma_{J/\psi g \rightarrow c\bar{c}} = 0.3$ fm 2 . For $m_c = 1.5$ GeV, which is smaller than the J/ψ production threshold, the destruction rate is a constant and the production rate increases with the temperature. The destruction rate is always larger than the production rate. As m_c increases, the production rate increases. When m_c is larger than the

J/ψ production threshold, the destruction rate decreases with increasing m_c . For $m_c = 1.7$ GeV, $\langle \sigma_{J/\psi g \rightarrow c\bar{c}} v \rangle$ starts from a value smaller than $\sigma_{J/\psi g \rightarrow c\bar{c}} c$. It increases with temperature to approach $\sigma_{J/\psi g \rightarrow c\bar{c}} c = 0.3$ fm²c. $\langle \sigma_{c\bar{c} \rightarrow J/\psi g} v \rangle$ has the same shape as the $m_c = 1.5$ GeV case and increases with the temperature of the plasma. It is smaller than the destruction rate up to $T = 0.7$ GeV. When $m_c = 1.87$ GeV, which is larger than the production threshold, the production rate is always larger than the destruction rate. The production rate for $m_c = 1.87$ GeV decreases as the temperature of the plasma increases, reflecting the decrease in the production cross section away from the threshold. We also plot the rates for the case with the dipole $J/\psi g \rightarrow c\bar{c}$ cross section determined by Eq. (10) in Fig. (3). $\langle \sigma_{c\bar{c} \rightarrow J/\psi g} v \rangle$ is still larger than $\langle \sigma_{J/\psi g \rightarrow c\bar{c}} v \rangle$. However, because the peak value of the dipole cross section is smaller than 0.3 fm², also because the cross section is exclusive and decreases with s , the rates are smaller than the constant cross section case shown in Fig. (3c).

C. Centrality and normalization

We will use the number of participants to characterize the centrality. The number of participants is calculated in the Glauber model with hard sphere geometry according to

$$\begin{aligned}
N_{part}(b) &= \int d\vec{s} (t_A(\vec{s} + \frac{\vec{b}}{2})(1 - \exp(-\sigma_{NN} t_B(\vec{s} - \frac{\vec{b}}{2}))) \\
&\quad + t_B(\vec{s} - \frac{\vec{b}}{2})(1 - \exp(-\sigma_{NN} t_A(\vec{s} + \frac{\vec{b}}{2})))) \\
&= 8\rho_N \int_0^{R-\frac{b}{2}} dx \int_0^{\sqrt{R^2 - (x + \frac{b}{2})^2}} dy (z_0(1 - \exp(-2\sigma_{NN} \rho_N z_0')) \\
&\quad + z_0'(1 - \exp(-2\sigma_{NN} \rho_N z_0))), \tag{11}
\end{aligned}$$

In the above, σ_{NN} is the nucleon-nucleon inelastic cross section. We will use $\sigma_{NN} = 40$ mb.

The J/ψ central rapidity density is normalized to the number of binary nucleon-nucleon collisions. We will plot $B \frac{dN_{J/\psi}}{dy}|_{y=0}/N_{coll}$, where $B = 0.06$ is the J/ψ to e^+e^- or $\mu^+\mu^-$ decay branching ratio, the number of binary nucleon-nucleon collisions is given by

$$\begin{aligned}
N_{coll}(b) &= \sigma_{NN} \int d\vec{s} t_A(\vec{s} + \frac{\vec{b}}{2}) t_B(\vec{s} - \frac{\vec{b}}{2}) \\
&= 4\rho_N^2 \sigma_{NN} \int_0^{R-\frac{b}{2}} dx \int_0^{\sqrt{R^2 - (x + \frac{b}{2})^2}} dy z_0 z_0'. \tag{12}
\end{aligned}$$

The number of participant nucleons and the number of binary nucleon-nucleon collisions are plotted in Fig. (4).

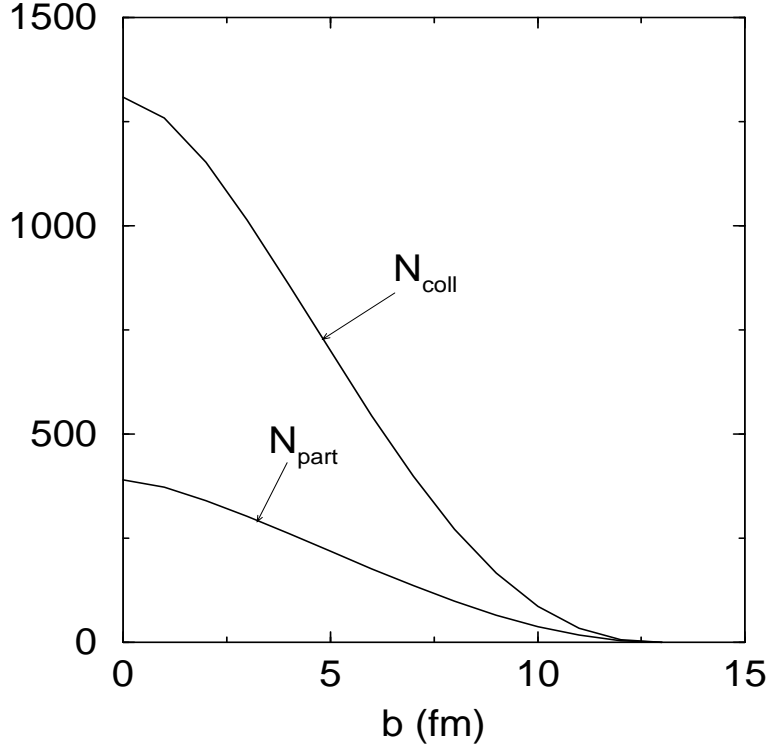


FIG. 4: The number of participant nucleons N_{part} and the number of binary nucleon-nucleon collisions N_{coll} as functions of the impact parameter.

D. Evolution of the gluon plasma

The evolution of the gluon plasma is described by the Bjorken model. We will use the latest freeze-out time τ_f to characterize the lifetime of the plasma. Fig. (5) shows that as the number of participant nucleons increases, the lifetime of the plasma increases. The typical lifetime for a plasma with an initial gluon rapidity density of 300 and a freeze-out temperature of 0.15 GeV is about 5 fm/c. Increasing the gluon rapidity density to 500 will bring the lifetime to about 8.5 fm/c, while increasing the freeze-out temperature to 0.17 GeV will decrease the lifetime to about 3.5 fm/c.

The temperature in the central transverse cell at the initial time as a function of the number of participating nucleons is shown in Fig. (6). It increases very rapidly when the number of participating nucleons goes from 0 to 50 and changes only slowly when the number of participating nucleons goes above 100. The typical initial temperature in the central cell is about 500 MeV.

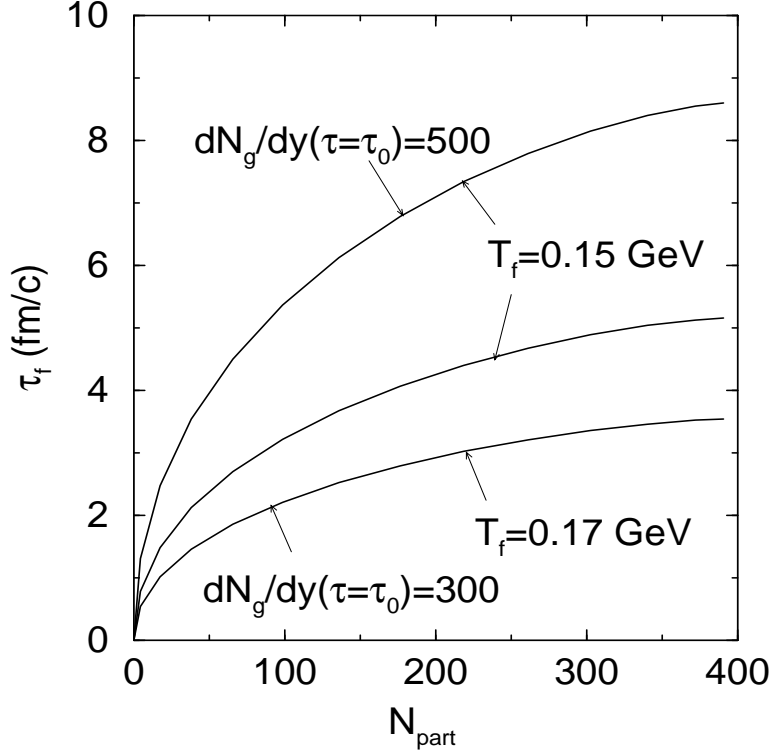


FIG. 5: Freeze-out time τ_f as a function of the number of participant nucleons N_{part} .

E. J/ψ production results

J/ψ enhancement was predicted by Thews *et. al* using the kinetic formation model. The PHENIX data excluded strong enhancement of the J/ψ particle. We are going to explore the possibility of J/ψ suppression from the kinetic formation model. About 10 $c\bar{c}$ pairs are produced on average in each Au-Au event. We assume no strong initial state energy loss of the produced $c\bar{c}$ pairs. The rapidity range of the $c\bar{c}$ pairs is taken to be $\Delta y = 4$. Now we vary the charm quark mass m_c , and observe the effect of changing the dynamical equilibrium of the J/ψ particle through the reactions $c\bar{c} \rightarrow J/\psi g$ and $J/\psi g \rightarrow c\bar{c}$.

The destruction of J/ψ or its precursor (the correlated $c\bar{c}$ pair that produces a J/ψ when there are no final state interactions) by collisions with incoming nucleons depends on the cross section $\sigma_{J/\psi N}$. When the colliding nuclei are highly Lorentz contracted at high enough energies, the nuclei pass through each other much earlier than the formation time of a J/ψ . The J/ψ particle will not be strongly suppressed by the incoming nucleons. We will use $\sigma_{J/\psi N} = 0$ to simulate this case. The centrality dependence of J/ψ yields are shown in Fig. (7). When $m_c=1.3, 1.5, 1.7$ GeV, the final J/ψ number is smaller than the

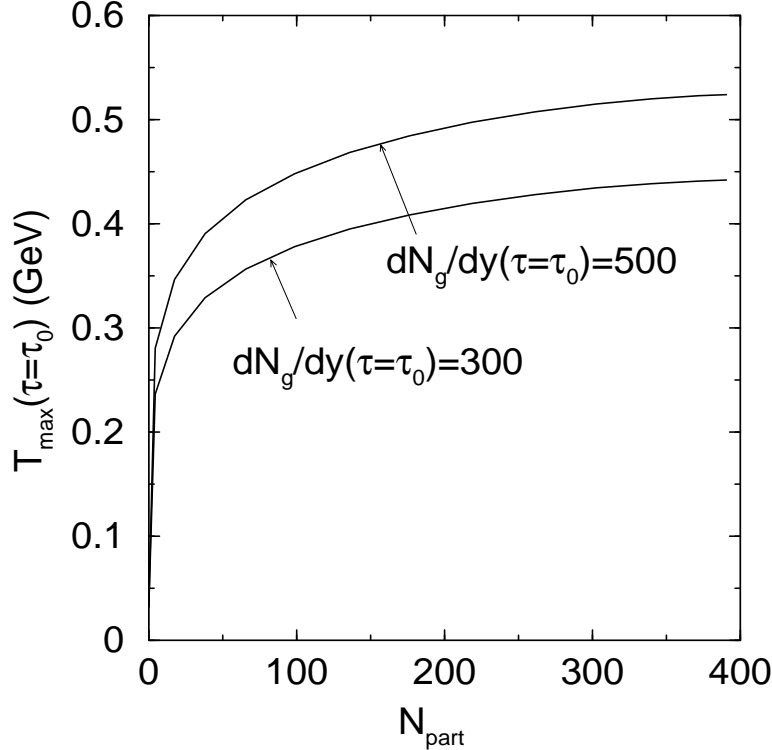


FIG. 6: Initial temperature of the center cell as a function of the number of participant nucleons N_{part} .

superposition of nucleon-nucleon collisions. The larger the cross section, the smaller the final J/ψ number. When the J/ψ destruction cross section $\sigma_{J/\psi g}$ goes up over about 5 mb, the curves converge. This gives the approximate dynamical equilibrium J/ψ value. The equilibrium value appears to be independent of centrality for mid-central and central Au-Au collisions. It increases with the charm quark mass m_c . Also notice that $m_c = 1.7$ GeV is larger than the J/ψ production threshold. However, the initial J/ψ is higher than the equilibrium value, and the final J/ψ number is smaller than the initial. For $m_c = 1.9$ GeV, The equilibrium value is larger than the initial J/ψ number and the final J/ψ number increases with increasing J/ψ gluon cross section. In the J/ψ suppression case, the final J/ψ number decreases with increasing centrality while in the J/ψ enhancement case, it increases with increasing centrality.

The adaptive step size Runge-Kutta method is used in solving the evolution equation. The transverse plane is divided into 20×40 cells (20 divisions in the x direction from $-(R - \frac{b}{2})$ to $R - \frac{b}{2}$, and 40 divisions in the y direction from $-\sqrt{R^2 - (\frac{b}{2})^2}$ to $\sqrt{R^2 - (\frac{b}{2})^2}$). Results are

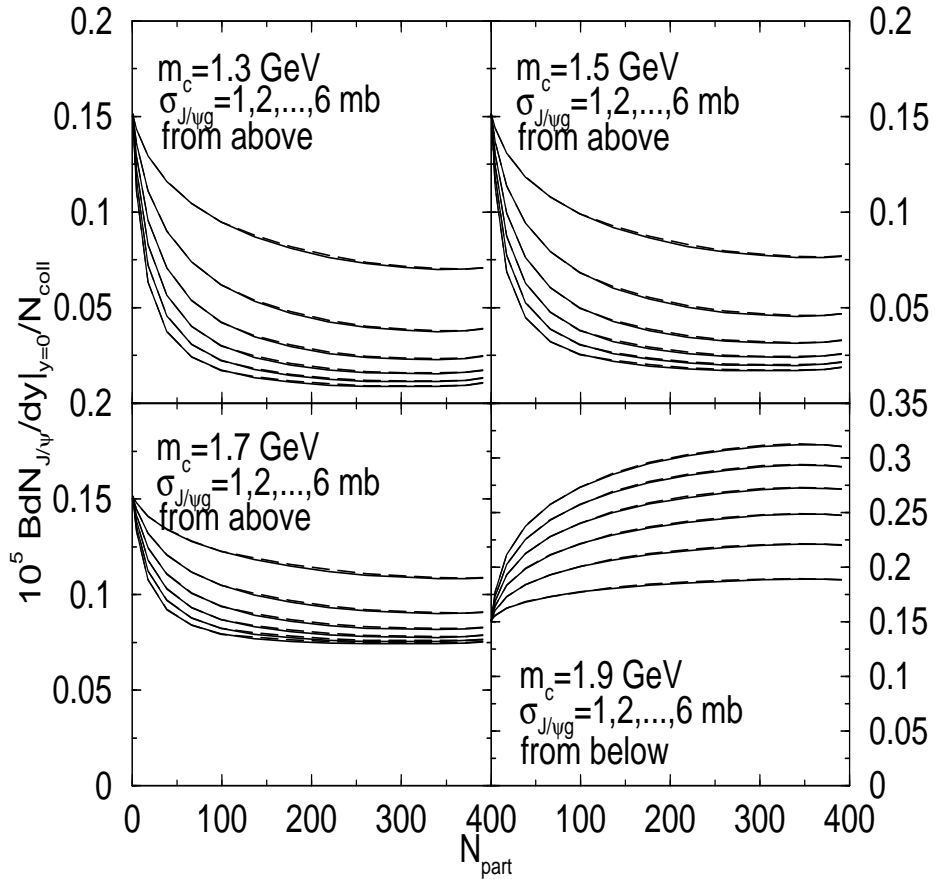


FIG. 7: Centrality dependence of J/ψ central rapidity density per binary nucleon-nucleon collision in Au-Au collisions when the suppression of J/ψ by incoming nucleons is negligible ($\sigma_{J/\psi N} = 0$). Solid lines are for 20×40 cells and dashed lines are for 10×20 cells.

shown in Fig. (7) as solid lines. Dashed lines are for the 10×20 cell division case. They agree well with the 20×40 cell division results.

At RHIC energies, the number of J/ψ is much smaller than the number of charm-anti-charm quark pairs. One can approximate the number of charm quarks at time τ by the initial number of charm quarks, and solve Eq. (3) to obtain the solution

$$N_{J/\psi}(\tau_f) = \epsilon(\tau_f, \tau_0) \left[N_{J/\psi}(\tau_0) + N_c^2(\tau_0) \int_{\tau_0}^{\tau_f} \frac{\lambda_F(\tau) d\tau}{V(\tau) \epsilon(\tau, \tau_0)} \right]. \quad (13)$$

Here,

$$\epsilon(\tau, \tau_0) = \exp \left\{ - \int_{\tau_0}^{\tau} \lambda_D(\tau') \rho_g(\tau') d\tau' \right\}. \quad (14)$$

The approximation solution gives no observable difference when the J/ψ production rate is small, for example, when $m_c = 1.3$ GeV. When the production rate is large, for example,

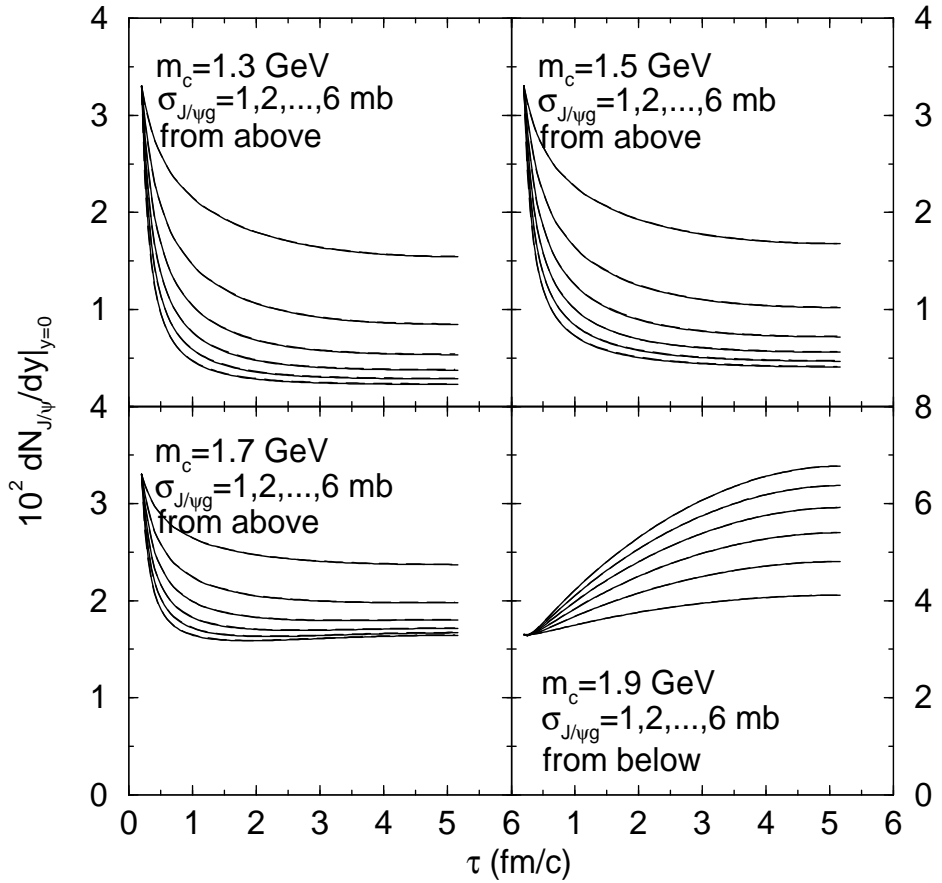


FIG. 8: J/ψ number evolution for central ($b = 0$) Au-Au collisions at $\sqrt{s_{NN}} = 200$ GeV.

when $m_c = 1.9$ GeV and $\sigma_{J/\psi g} = 6$ mb, it can overestimate the J/ψ yield (relative to the exact solution) by about 4%.

We show the time evolution of J/ψ number in central ($b = 0$) collisions in Fig. (8). When $m_c = 1.3, 1.5, 1.7$ GeV, the J/ψ number changes drastically before $\tau = 1$ fm/c. When $m_c = 1.7$ GeV and $\sigma_{J/\psi g} = 5, 6$ mb, the J/ψ value reaches the lowest point at about 1 fm/c, then it increases slightly. This is because of the production of J/ψ in central cells. For $m_c = 1.9$ GeV, the J/ψ number changes over the entire evolution. The equilibration time is larger than the system lifetime and results with different $\sigma_{J/\psi g}$ values do not converge and dynamical equilibrium of J/ψ has not been reached over the evolution.

To check the sensitivity on parameters, we change the gluon rapidity density from 300 to 500. Results are shown in Fig. (9). As the initial gluon number increases, the initial temperature increases, more J/ψ 's will be destructed during the evolution. This leads to an

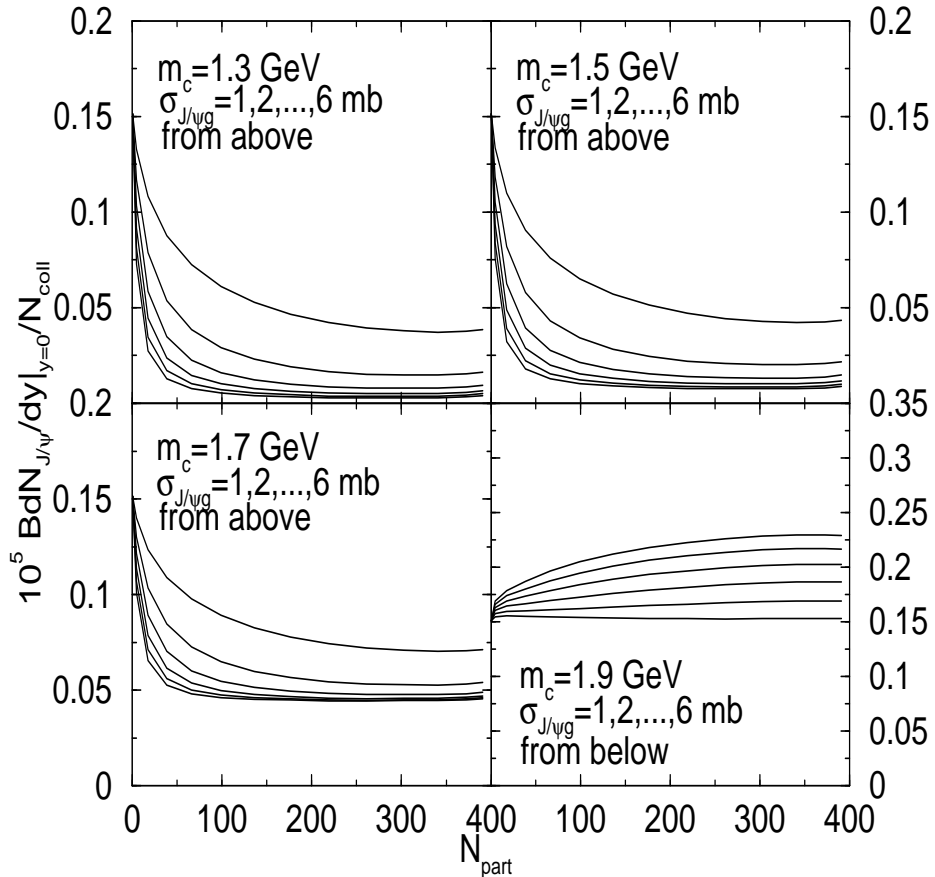


FIG. 9: Centrality dependence of J/ψ central rapidity density per binary nucleon-nucleon collision when $\sigma_{J/\psi N} = 0$ mb and $dN_g/dy(b = 0) = 500$.

overall decrease of the J/ψ yield for all charm mass values. If we keep the gluon rapidity density to be 300 and increase the freeze-out temperature from 0.15 GeV to 0.17 GeV, no significant changes show up for $m_c = 1.3, 1.5, 1.7$ GeV as seen from Fig. (10). This indicates that the equilibration time is much longer than the time that goes from $T = 0.17$ GeV to $T = 0.15$ GeV. For the $m_c = 1.9$ GeV case, especially for large $\sigma_{J/\psi g}$ values, the final J/ψ values decrease significantly. For example, when $\sigma_{J/\psi g} = 6$ mb, the final J/ψ value for central collisions decreases from 0.31 to about 0.22. This shows that for the $m_c = 1.9$ GeV case, the final J/ψ value is still far from equilibrium and the equilibration time is not negligible compared with the time that goes from $T = 0.17$ GeV to $T = 0.15$ GeV.

To see the difference between the constant $\sigma_{J/\psi g \rightarrow c\bar{c}}$ case and the dipole form $\sigma_{J/\psi g \rightarrow c\bar{c}}$ specified in Eq. (10), we show the centrality dependence of J/ψ production in Fig. (11).

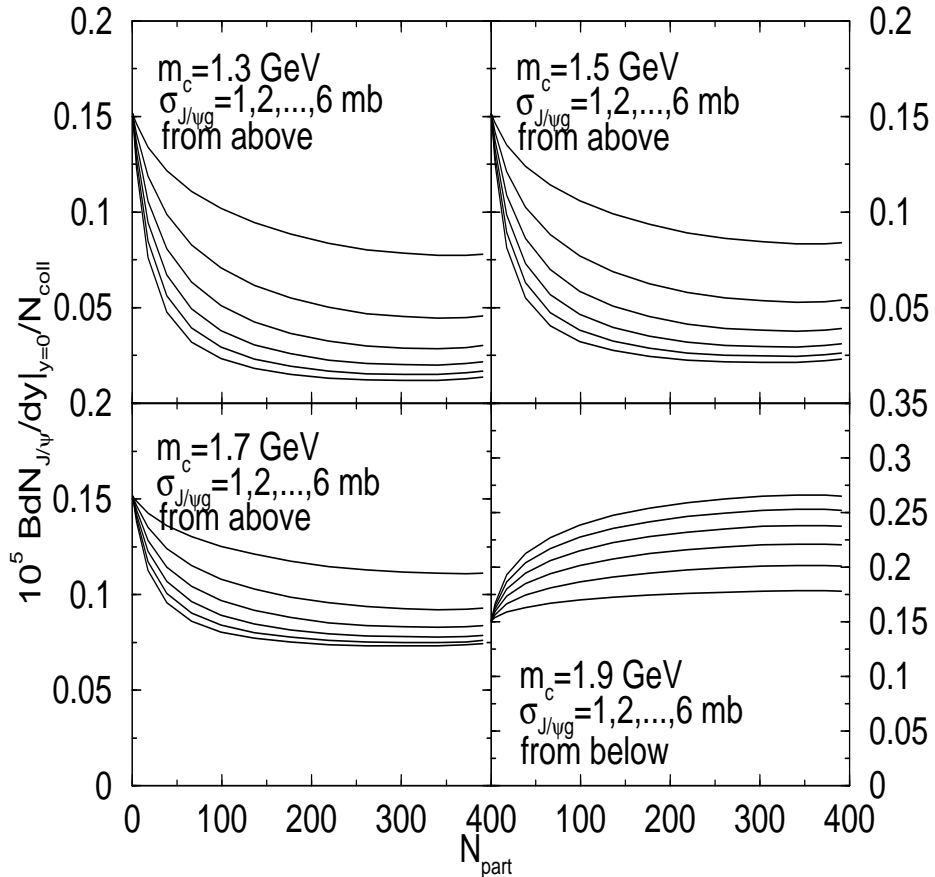


FIG. 10: Centrality dependence of J/ψ central rapidity density per binary nucleon-nucleon collision when $\sigma_{J/\psi N} = 0$ mb and $T_f = 0.17$ GeV.

The J/ψ centrality dependence in the dipole cross section case follows closely the constant cross section case. It is between the two curves with $\sigma_{J/\psi g \rightarrow c\bar{c}} = 1.0$ mb and $\sigma_{J/\psi g \rightarrow c\bar{c}} = 2.0$ mb. The peak value of the dipole cross section is about 2 mb. The J/ψ yield is smaller than the constant 2 mb destruction cross section case because the dipole cross section does not have destruction by high energy gluons with additional radiation involved. The enhancement relative to the superposition of nucleon-nucleon production when $\sigma_{J/\psi g \rightarrow c\bar{c}} = 2.0$ mb is about 1.2 times larger than the enhancement when the dipole cross section is used, independent of centrality. In other words, the dipole cross section case can be described by the constant cross section case with an effective K factor. We notice that the dipole cross section and the constant cross section have very different dependences on the center-of-mass energy (Fig. 2). The above comparison indicates that the centrality dependence of J/ψ production reflects

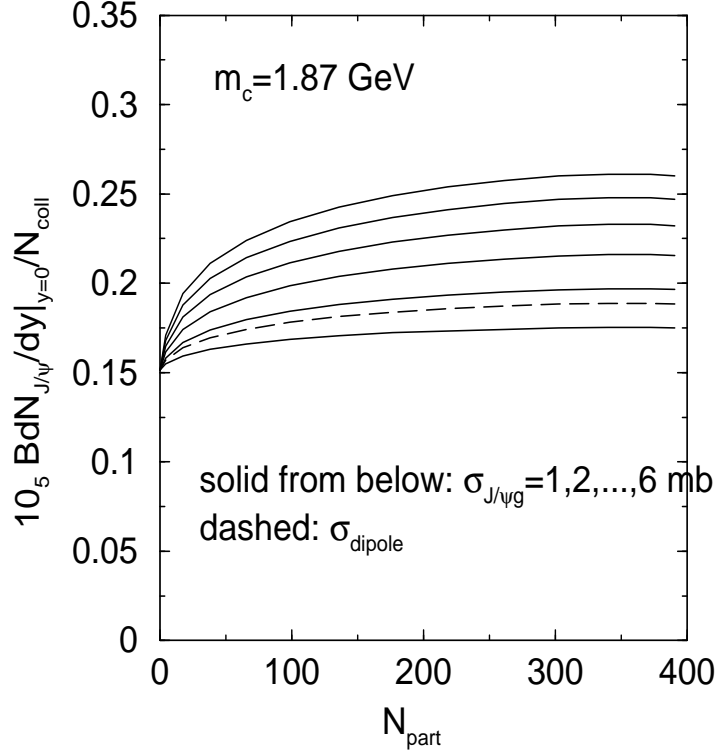


FIG. 11: Centrality dependence of J/ψ central rapidity density per binary nucleon-nucleon collision when for $m_c = 1.87$ GeV.

the overall production rate and can not differentiate between detailed cross section shapes.

Now we add in the Glauber suppression of J/ψ . We will first look at the $\sigma_{J/\psi N} = 4.4$ mb case. For $m_c = 1.3, 1.5$, and 1.7 GeV, the final J/ψ values are still smaller than the initial values as shown in Fig. (12). Because of the destruction by incoming nucleons, the final J/ψ values and the initial are closer. For $m_c = 1.9$ GeV, the final J/ψ values first decrease with centrality and then increase with centrality. This centrality dependence differs from the monotonic centrality dependence when $m_c = 1.3, 1.5, 1.7$ GeV. Because of suppression by the incoming nucleons, when $\sigma_{J/\psi g}$ is small, the final J/ψ values are no longer larger than the superposition of J/ψ from nucleon-nucleon collisions. If $\sigma_{J/\psi N}$ is further increased to 7.1 mb, the initial J/ψ number after collisions with incoming nucleons is even smaller as shown in Fig. (13). The range between the initial and final J/ψ values decreases for the $m_c = 1.3, 1.5$ GeV cases. For the $m_c = 1.7$ GeV case, it goes below the equilibrium value and the final state J/ψ equilibration increases the J/ψ yield. When $m_c = 1.9$ GeV, the range between initial and equilibrium increases.

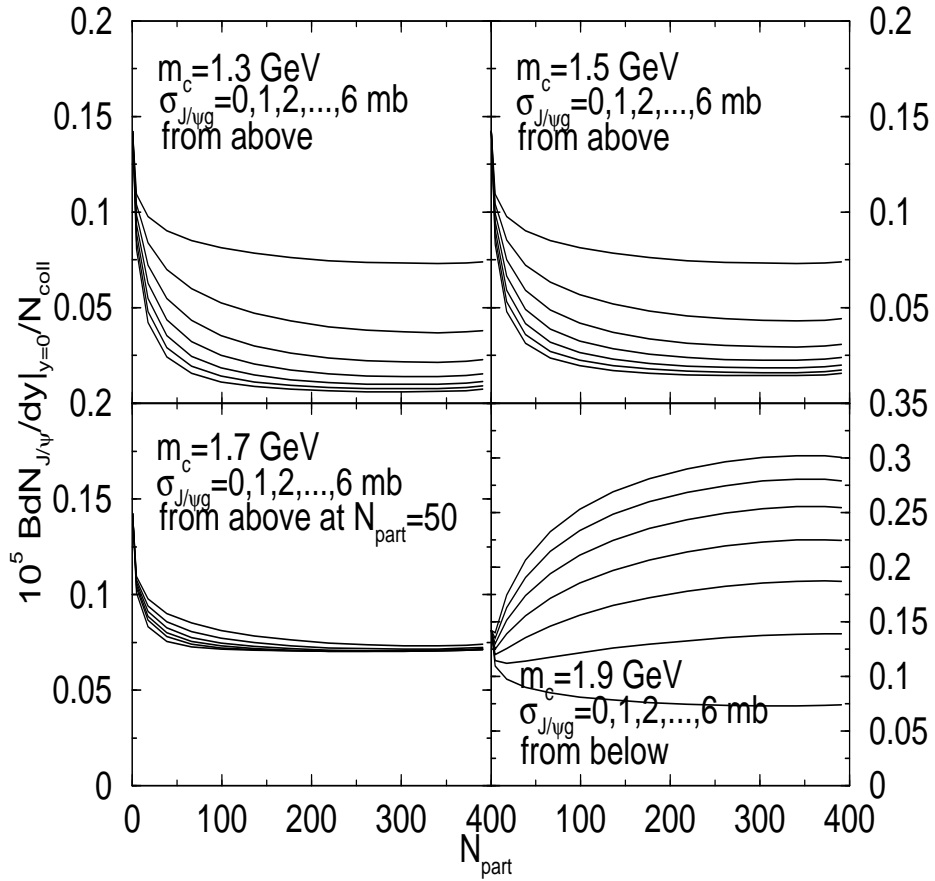


FIG. 12: Centrality dependence of J/ψ central rapidity density per binary nucleon-nucleon collision when $\sigma_{J/\psi N} = 4.4$ mb.

IV. SUMMARY AND CONCLUSIONS

The J/ψ production in Au-Au collisions at $\sqrt{s_{NN}} = 200$ GeV is studied in the framework of the kinetic formation model. It is shown that when the charm quark mass m_c is smaller than some critical value, the J/ψ yield monotonically decreases with increasing centrality. As $\sigma_{J/\psi g \rightarrow c\bar{c}}$ increases, the final J/ψ yield moves away from the value right after the Glauber suppression by the incoming nucleons and approaches the dynamical equilibrium value. The J/ψ production data from d-Au collisions at the Relativistic Heavy Ion Collider will help to fix the Glauber suppression and the higher statistics Au-Au data will further help to understand J/ψ -charm equilibration.

The current model does not have gluon nuclear shadowing. Further inclusion of shadowing will decrease the number of charm quarks produced and lower the number of J/ψ 's produced.

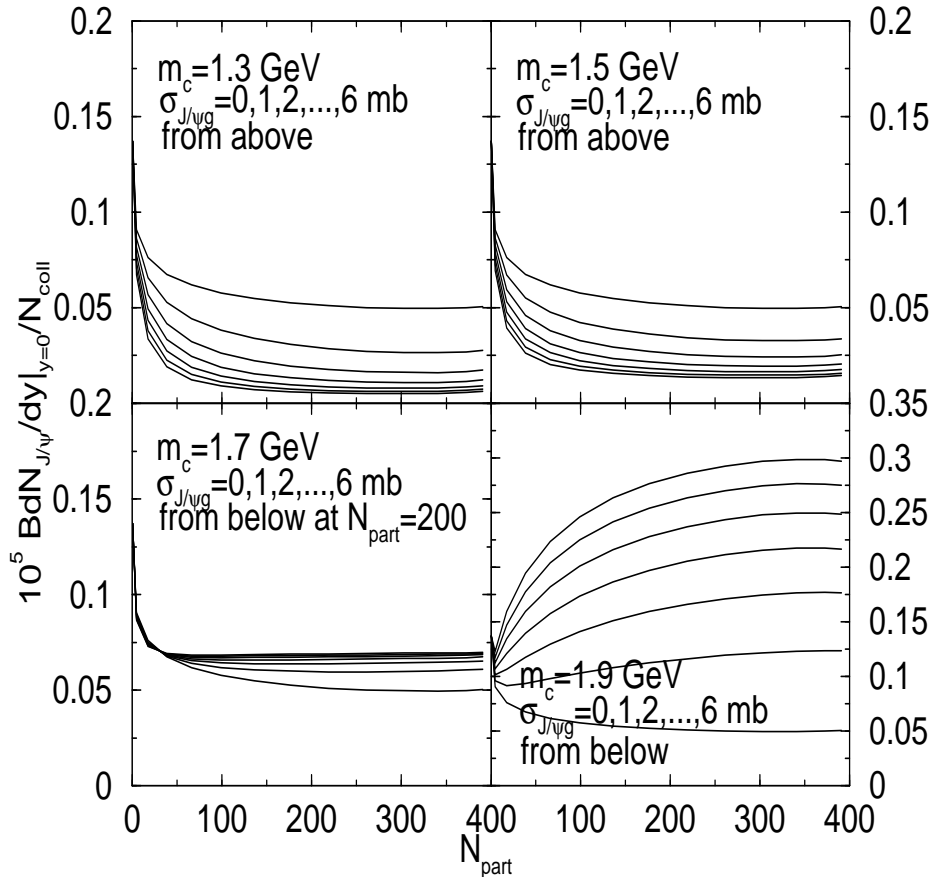


FIG. 13: Centrality dependence of J/ψ central rapidity density per binary nucleon-nucleon collision when $\sigma_{J/\psi N} = 7.1$ mb.

Color screening [4, 67, 68, 69] will lead to more dissociation of J/ψ and more suppression of final J/ψ yield. The inclusion of feeddown will lead to the same effect as higher charmonium resonances are easier to be dissociated. Transverse expansion will lead to earlier freeze-out and should not change the qualitative feature of J/ψ suppression. J/ψ -charm equilibration in the hadron phase is beyond the scope of this paper. However, as the equilibrium value in the hadron phase is smaller than the superposition of production from nucleon-nucleon collisions, equilibration in the hadron phase will also lead to J/ψ suppression in Au-Au collisions.

Acknowledgments

We thank B.A. Li and Z. Lin for helpful discussions. We also thank B. Hemphill and T. Franks for participation in the early stage of the study. This work is supported by the U.S. National Science Foundation under Grant No. PHY-0140046, and the Arkansas Science and Technology Authority under Grant No. 01-B-20.

- [1] B. Müller, *Rep. Prog. Phys.* **58**, 611 (1995).
- [2] S.A. Bass, M. Gyulassy, H. Stöcker, and W. Greiner, *J. Phys. G* **25**, R1 (1999).
- [3] Proceedings of 16th International Conference on Ultra-Relativistic Nucleus-Nucleus Collisions (Quark Matter 2002), *Nucl. Phys.* **A715**.
- [4] T. Matsui and H. Satz, *Phys. Lett. B* **178**, 416 (1986).
- [5] E772 Collaboration (D.M. Alde *et al.*), *Phys. Rev. Lett.* **66**, 133 (1991).
- [6] E866/NuSea Collaboration (M. Leitch *et al.*), *Phys. Rev. Lett.* **84**, 3256 (2000).
- [7] NA 50 Collaboration (M.C. Abreu *et al.*), *Phys. Lett. B* **410**, 337 (1997).
- [8] E.V. Shuryak, *Sov. J. Nucl. Phys.* **28**, 408 (1979).
- [9] X.M. Xu, D. Kharzeev, H. Satz, and X.N. Wang, *Phys. Rev. C* **53**, 3051 (1996).
- [10] S. Gavin and R. Vogt, *Phys. Rev. Lett.* **78**, 1006 (1997).
- [11] D. Kharzeev, C. Lounrenco, M. Nardi, and H. Satz, *Zeit. Phys. C* **74**, 307 (1997).
- [12] W. Cassing and C.M. Ko, *Phys. Lett. B* **396**, 39 (1997).
- [13] C. Gale, S. Jeon, and J. Kapusta, *Phys. Lett. B* **459**, 455 (1999).
- [14] J. Geiss, C. Greiner, E.L. Bratkovskaya, W. Cassing, and U. Mosel, *Phys. Lett. B* **447**, 31 (1999).
- [15] D.E. Kahana, S.H. Kahana, *Phys. Rev. C* **59**, 1651 (1999).
- [16] B.H. Sa, A. Tai, H. Wang, and F.H. Liu, *Phys. Rev. C* **59**, 2728 (1999).
- [17] C. Spieles, R. Vogt, L. Gerland, S.A. Bass, M. Bleicher, H. Stöcker, and W. Greiner, *Phys. Rev. C* **60**, 054901 (1999).
- [18] R. Vogt, *Phys. Rep.* **310**, 197 (1999).
- [19] J.P. Blaizot, P. M. Dinh, J.Y. Ollitrault, *Phys. Rev. Lett.* **85**, 4012 (2000).
- [20] A. Capella, E.G. Ferreiro, and A.B. Kaidalov, *Phys. Rev. Lett.* **85**, 2080 (2000).

- [21] C. Gale, S. Jeon, J. Kapusta, Phys. Rev. C **63**, 024901 (2001).
- [22] NA50 Collaboration (M.C. Abreu *et al.*), Phys. Lett. B **477**, 28 (2000).
- [23] R.L. Thews, M. Schroedter, and J. Rafelski, Phys. Rev. C **63**, 054905 (2001).
- [24] P. Braun-Munzinger and J. Stachel, Phys. Lett. B **490**, 196 (2000).
- [25] M.I. Gorenstein, A.P. Kostyuk, H. Stöcker, and W. Greiner, Phys. Lett. B **509** 277 (2001).
- [26] L. Grandchamp and R. Rapp, Phys. Lett. B **523**, 60 (2001).
- [27] B. Zhang, C.M. Ko, B.A. Li, Z. Lin, B.H. Sa, Phys. Rev. C **62**, 054905 (2000).
- [28] M.I. Gorenstein, A.P. Kostyuk, H. Stöcker, and W. Greiner, Phys. Lett. B **524** 265 (2002).
- [29] L. Grandchamp and R. Rapp, Nucl. Phys. A **709**, 415 (2002).
- [30] B. Zhang, C.M. Ko, B.A. Li, Z.W. Lin, and S. Pal, Phys. Rev. C **65**, 054909 (2002).
- [31] B. Zhang, B.A. Li, A.T. Sustich, and C. Teal, Phys. Lett. B **546**, 63 (2002).
- [32] A. Andronic, P. Braun-Munzinger, K. Redlich, J. Stachel, Phys. Lett. B **571**, 36 (2003).
- [33] E.L. Bratkovskaya, W. Cassing, H. Stocker, Phys. Rev. C **67**, 054905 (2003).
- [34] L. Grandchamp, R. Rapp, G.E. Brown, e-Print archive: hep-ph/0306077.
- [35] PHENIX Collaboration (S.S. Adler *et al.*), Phys. Rev. Lett. **92**, 051802 (2004).
- [36] PHENIX Collaboration (S.S. Adler *et al.*), Phys. Rev. C **69**, 014901 (2004).
- [37] N. Brambilla, Y. Sumino, and A. Vairo, Phys. Lett. B **513**, 381 (2001).
- [38] M. Eidemüller and M. Jamin, Phys. Lett. B **498**, 203 (2001).
- [39] S. Recksiegel and Y. Sumino, Phys. Rev. D **67**, 014004 (2003).
- [40] S. Rechsiegel and Y. Sumino, Phys. Lett. B **578**, 369 (2004).
- [41] E.J. Eichten and C. Quigg, Phys. Rev. D **49**, 5845 (1994).
- [42] R.V. Gavai, S. Gupta, P.L. McGaughey, E. Quack, P.V. Ruuskanen, R. Vogt, and X.N. Wang, Int. J. Mod. Phys. A **10**, 2999 (1995).
- [43] G. Altarelli, M. Diemoz, G. Martinelli, and P. Nason, Nucl. Phys. **B308**, 724 (1988).
- [44] M.E. Peskin, Nucl. Phys. **B156**, 365 (1979).
- [45] G. Bhanot and M.E. Peskin, Nucl. Phys. **B156**, 391 (1979).
- [46] PHENIX Collaboration (K. Adcox *et al.*), Phys. Rev. Lett. **88**, 192303 (2002).
- [47] Y.L. Dokshitzer and D.E. Kharzeev, Phys. Lett. B **519**, 199 (2001).
- [48] S. Batsouli, S. Kelly, M. Gyulassy, and J.L. Nagle, Phys. Lett. B **577**, 26 (2003).
- [49] M. Djordjevic and M. Gyulassy, Phys. Lett. B **560**, 37 (2003).
- [50] M. Djordjevic and M. Gyulassy, Phys. Rev. C **68**, 034914 (2003).

- [51] B.W. Zhang, E. Wang, and X.N. Wang, e-Print archive: nucl-th/0309040.
- [52] M. Djordjevic and M. Gyulassy, Nucl. Phys. **A733**, 265 (2004).
- [53] D. Kharzeev and K. Tuchin, Nucl. Phys. **A735**, 248 (2004).
- [54] A.D. Martin, R.G. Roberts, W.J. Stirling, and R.S. Thorne, Eur. Phys. J. C **23**, 73 (2002).
- [55] K.J. Eskola, Nucl. Phys. **A590**, 383c (1995).
- [56] X.N. Wang, Phys. Rept. **280**, 287 (1997).
- [57] P. Lévai, B. Müller, and X.N. Wang, Phys. Rev. C **51**, 3326 (1995).
- [58] Z. Lin and M. Gyulassy, Phys. Rev. C **51**, 2177 (1995).
- [59] Z.W. Lin and M. Gyulassy, Nucl. Phys. **A590** 495c (1995).
- [60] B. Svetitsky, Phys. Rev. D **37**, 2484 (1988).
- [61] J.D. Bjorken, Phys. Rev. D **27**, 140 (1983).
- [62] X.N. Wang and M. Gyulassy, Phys. Rev. D **44**, 3501 (1991).
- [63] M. Gyulassy and X.N. Wang, Comput. Phys. Commun. **83**, 307 (1994).
- [64] J.L. Nagle and M.J. Bennett, Phys. Lett. B **465**, 21 (1999).
- [65] M.J. Bennett, J.L. Nagle, Phys. Rev. C **59**, 2713 (1999).
- [66] NA50 Collaboration (L. Ramello *et al.*), Nucl. Phys. **A715**, 243 (2003).
- [67] S. Datta, F. Karsch, P. Petreczky, and I. Wetzorke, Nucl. Phys. Proc. Suppl. **119**, 487 (2003).
- [68] T. Umeda, H. Matsufuru, O. Miyamura, and K. Nomura, Nucl. Phys. **A721**, 922 (2003).
- [69] M. Asakawa and T. Hatsuda, Phys. Rev. Lett. **92**, 012001 (2004).